



UNIVERSITATEA DIN
BUCUREȘTI
VIRTUTE ET SAPIENTIA

FACULTY OF CHEMISTRY

DEPARTMENT OF INORGANIC CHEMISTRY

MSc Thesis - literature report

**Crystalline Porous Coordination Polymers with
Catalytic / Gas Adsorption Properties**

Master Program: CHEMISTRY OF ADVANCED MATERIALS

MSc Student: MIHAI BORDEIAȘU

MSc Thesis Advisor: Assist. Prof. Dr. DELIA-LAURA POPESCU

February 7, 2020

Content

Introduction	2
1. Structural features and physical properties of crystalline porous coordination polymers	3
1.1. Connectors and linkers used in synthesis of porous coordination polymers	3
1.2. Dimensionality and motifs of porous coordination polymers	4
1.3. Porosity of porous coordination polymers	5
1.4. Flexibility of porous coordination polymers	6
2. Applications of porous coordination polymers	7
2.1. Catalysis	7
2.1.1. Functional organic sites	7
2.1.2. Incorporation of nanocatalysts	9
2.1.3. Immobilization of unsaturated metal sites	11
2.2. Gas storage	12
2.2.1. Carbon dioxide storage	13
2.2.2. Hydrogen storage	15
2.2.3. Hydrocarbons storage	16
2.2.4. Toxic gases storage	18
Objectives of the MSc Thesis	21
References	22

Introduction

This report represents the theoretical background for the dissertation topic in which we want to conduct a study on the gas adsorption and catalytic properties of crystalline porous coordination polymers (PCPs). In order to have a better understanding of the PCPs application areas, it is crucial to understand the structural features and the physico-chemical properties of the coordination polymers, along with the influence of their intrinsic characteristics on the various topologies and behavior of this class of compounds.

Porous coordination polymers, most commonly known as metal-organic frameworks (MOFs), are a class of porous materials formed by self-assembly of metal ions or clusters and organic ligands yielding to an infinite structure with high regularity, tunable pore sizes, high surface area and adjustable internal surface properties [1,2].

A great advantage of this class of compounds is their diversity; there can be obtained different types of coordination polymers depending on the nature of the construction units and their properties which have a major impact on PCPs topology, defining the coordination polymers.

Due to their interesting properties, which leads to versatile architectures, porous coordination polymers are used in different applications (Fig.1.), such as adsorption, separation, and storage of gases, heterogeneous catalysis, drug delivery and sensor technology, magnetism, luminescence and non-linear optics [3].



Fig.1. Applications of porous coordination polymers

1. Structural features and physical properties of porous coordination polymers

1.1. Connectors and linkers used in synthesis of PCPs

The building blocks of coordination polymers are the metal ions or clusters, which act as *connectors*, and organic ligands, which form the bridges between connectors [4]. Connectors have different shapes and sizes depending on the stereochemistry of the metal ion, its size, hardness/softness [5], influencing the dimensionality and structural motifs of the obtained coordination polymer. The tetrahedral and octahedral geometries are widely used because of their tendency to form 3D-architectures.

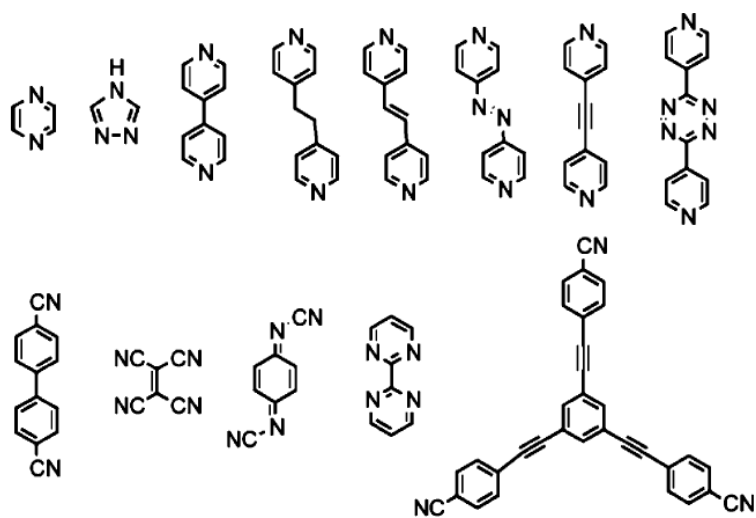


Fig.2. Neutral ligands

Source: Robin, A.Y., Fromm, K.M. Coord. Chem. Rev., 250(15-16) (2006), 2127–2157.

Organic, organometallic, and coordinative ligands act as linking groups between metal ions or clusters [5] and are called *spacers* or *linkers*. They have to be multidentate exo-type ligands in order to obtain the extended network of the coordination polymer. Linkers differ from one another in charge, the most common being the neutral (Fig.2.) and anionic (Fig.3.) ligands, as well as the core of these organic compounds, having different lengths and shapes [4,5]. Most of the ligands have aromatic rings in order to increase the rigidity of the final structure.

Besides the building blocks, counter ions and solvent molecules may be present in the structure, influencing the metal ion environment and/or acting as guest molecules in the free

space of the coordination polymer being involved in the weak interactions in the final solid state packing [4-6].

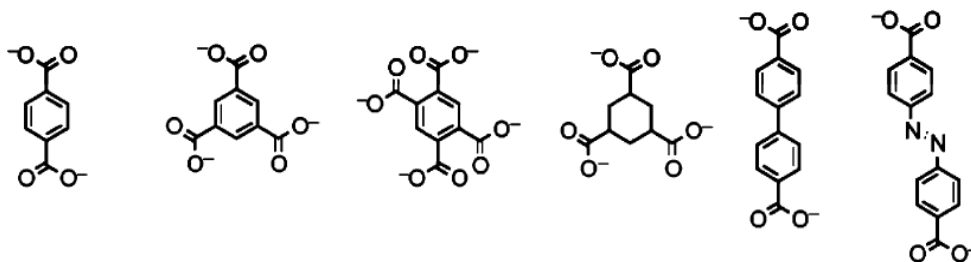


Fig.3. Anionic ligands

Source: Robin, A. Y., Fromm, K.M. *Coord. Chem. Rev.*, 250(15-16) (2006), 2127–2157.

1.2. Dimensionality and motifs

The dimensionality of the porous coordination polymers is represented in Figure 4. Dimensionality is determined in most of the cases by the coordination number of the metal, a 1D or 2D coordination polymer being formed by using metals with low coordination number and a 3D-framework by metals with higher coordination number [4]. Therefore, it is easy to predict and control the dimensionality, as well as the structural motifs, of a coordination polymer by using the proper metal.

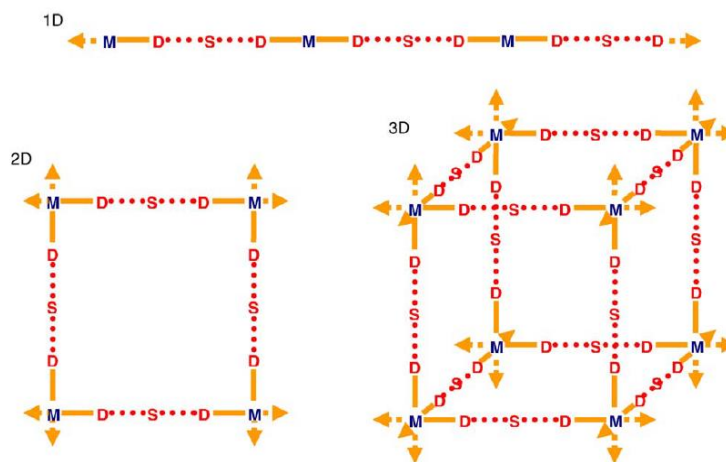


Fig.4. Dimensionality of the porous coordination polymers

Source: Robin, A. Y., Fromm, K.M. *Coord. Chem. Rev.*, 250(15-16) (2006), 2127–2157

Motifs describe the arrangement of metal ions and organic ligands within the structure of the coordination polymers (Fig.5.), based on the stereochemistry of the metal and the number of coordinated ligands. As such, for 1D-motifs, the metal atom is coordinated by two divergent ligands, leading to infinite chains, while in the 2D-motifs there are three or four ligand molecules coordinated to the metal ion which expand on two directions [5]. 3D-motifs

are formed using four or six ligands depending on the geometry of the metal which in most of the cases is tetrahedral or octahedral. As shown in Figure 5, the most common motifs known for 1D PCPs are: linear, zigzag, double chain, helix, ladder, fish bone, and railroad; for 2D – honeycomb, brickwall, herringbone, bilayer; and for 3D – diamondoid, octahedral etc.

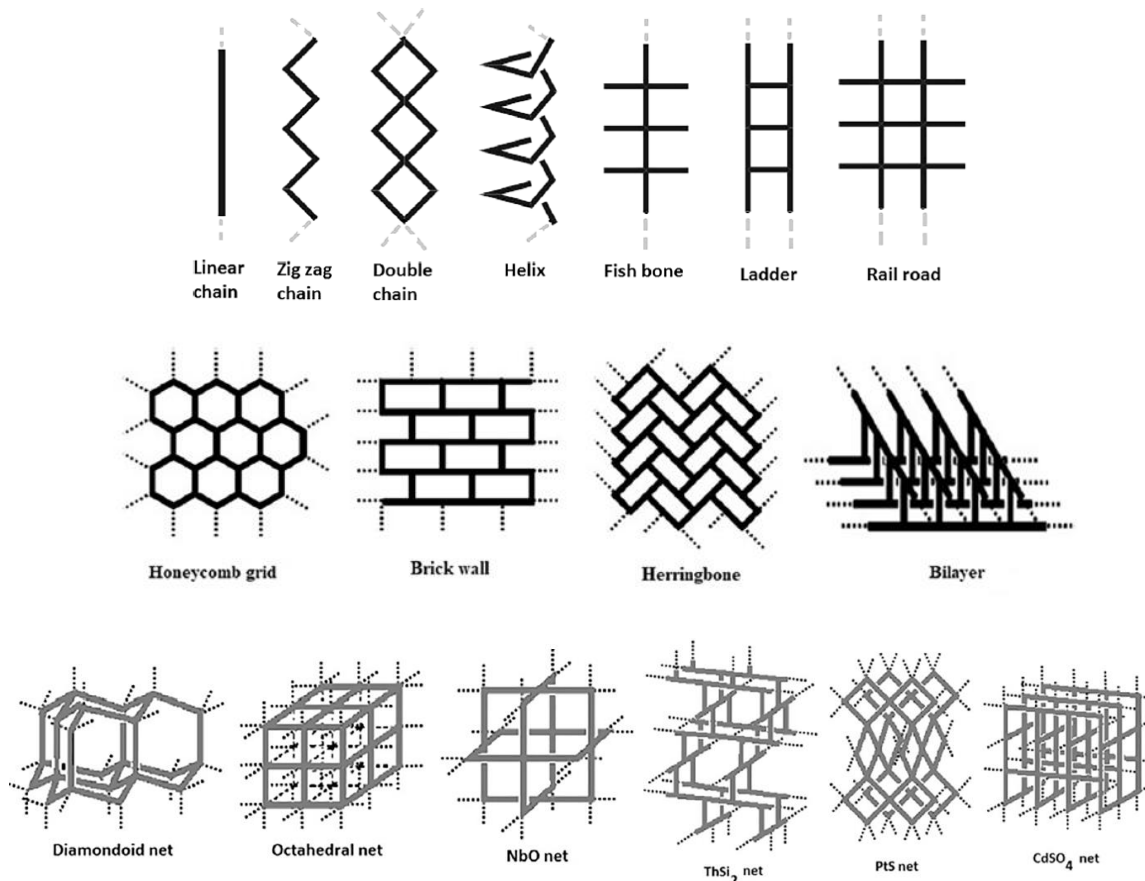


Fig.5. 1D (top), 2D (middle) and 3D (bottom) motifs of coordination polymers

Source: Ghosh, A., Hazra, A., Mondal, A., Banerjee, P., *Inorg. Chim. Acta*, 488 (2019), 86-119

1.3. Porosity

Porosity is essential in designing high performance materials mainly for storage, due to the empty space that is formed, but also for catalysis because it is providing a high surface area which is important for the catalytic process. Another application determined by the porosity is the separation and coordination polymers may be used in separation processes in the same fashion as zeolites. Due to its importance for previously mentioned applications, many studies focused on the increase of the porosity limit while maintaining the robustness of the polymer [7].

The easiest control of the pore size can be obtained by varying ligands length within the same type of network [8]. For large pore sizes it may be possible for the structure to

collapse in the absence of a guest molecule or at its removal, the catenation effect may occur, in which interpenetrating structures are formed in order to minimize the free space in the packing of the constituent particles in solids.

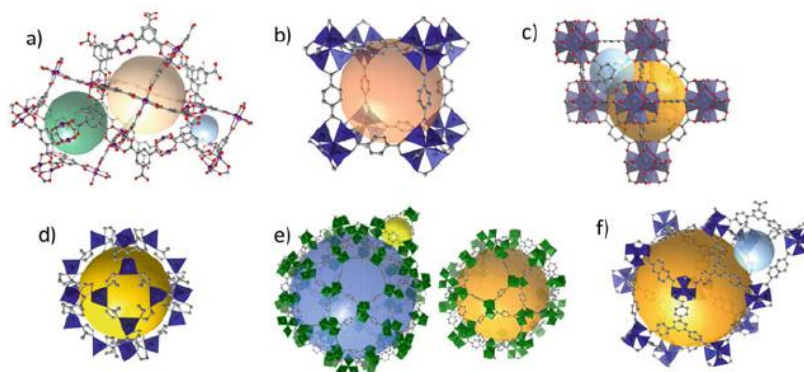


Fig.6. Pore structures in HKUST-1 (a), MOF-5 (b), UiO-66 (c), ZIF-8 (d), MIL-101 (e), DUT-6 (f)
 Source: Bon, V., Senkovska, I., Kaskel, S., Chapter 6: Metal-Organic Frameworks in K. Kaneko, F. Rodríguez-Reinoso (eds.), Nanoporous Materials for Gas Storage, Green Energy and Technology, (2019) 137–172

1.4. Flexibility

Flexibility is the property of porous coordination polymers to reversibly change their structure upon applying external stimuli, such as: guest molecules, heat, an electro-magnetic field, giving an advantage to these compounds over the other porous materials (zeolites and activated carbon). Guest molecules are the main factor that influences flexibility of PCPs, and can be classified into - rotation of bridging ligands (a), shape fitting response (b) or interpenetration (c), as can be seen in Figure 7 [9].

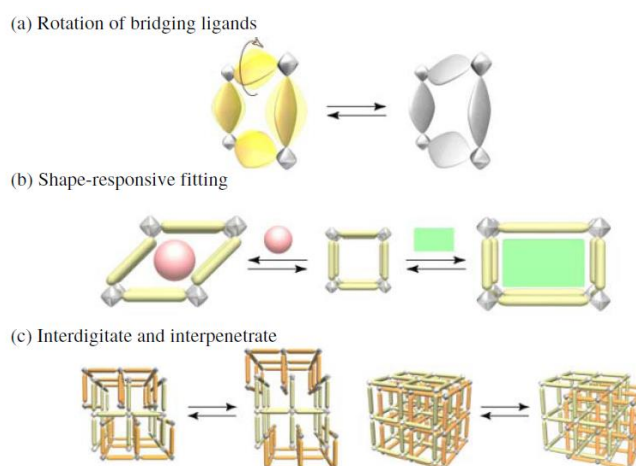


Fig.7. Schematic representation of PCPs flexible property

Source: Bureekaew, S., Shimomura, S., Kitagawa, S., Sci. Technol. Adv. Mater., 9(1) (2008), 014108

2. Applications

2.1. Catalysis

Porous coordination polymers (PCPs) are used in catalysis due to their unique features and although these compounds do not expose many coordinatively unsaturated metal sites, which could act as active catalytic sites, alternatives are used to prepare PCP-based type catalysts. Amongst these, the most accessible are: the use of functional organic sites [11], incorporation of nanocatalysts [12] or the structural modification in order to add unsaturated coordinative metal sites [13].

2.1.1. Functional organic sites

Hasegawa *et al.* [11] underlined the importance of functional organic sites (FOS) by using a tridentate ligand containing three amide groups (Figure 8) to develop a PCP catalyst and use it in a Knoevenagel condensation reaction to characterize its base-type properties.

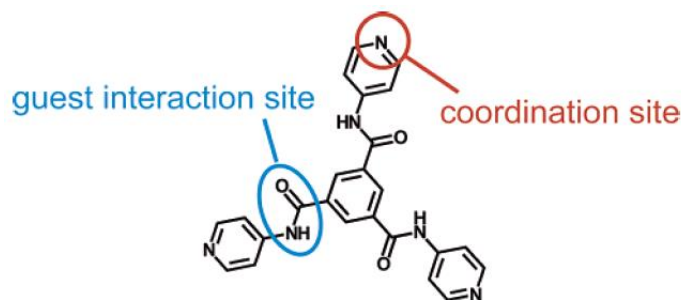


Fig.8. Structure of 1,3,5-Benzene Tricarboxylic Acid Tris[N-(4-pyridyl)amide] (4-btapa)
 Source: Hasegawa, S., Horike, S., Matsuda, R., Furukawa, S., Mochizuki, K., Kinoshita, Y., Kitagawa, S., *J. Am. Chem. Soc.*, 129(9) (2007), 2607–2614

The synthesized compound, $\{[\text{Cd}(4\text{-btapa})_2(\text{NO}_3)_2] \cdot 6\text{H}_2\text{O} \cdot 2\text{DMF}\}_n$, contains Cd^{2+} ions coordinated by six pyridil nitrogen atoms from different ligands forming an octahedral geometry (Figure 9). The arrangement of connectors and linkers generates six-membered ring composed of three octahedral $\text{Cd}(\text{II})$ and three 4-btapa units which interpenetrates to form three-dimensionality channels in the crystalline structure (Figure 10) [11].

The amide group is a functional group that has two types of hydrogen-bonding sites: the $-\text{NH}$ part which acts as electron acceptor and the $-\text{C}=\text{O}$ part as electron donor and are working as interaction sites with the substrate during the catalytic process.

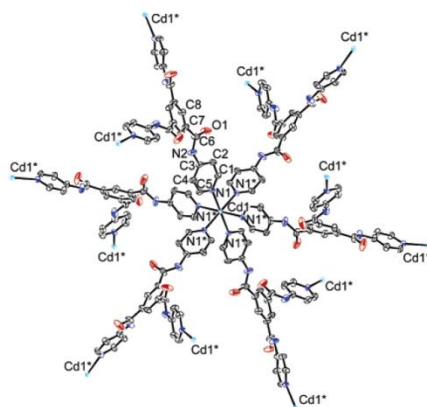


Fig.9. ORTEP drawing of $\{[\text{Cd}(4\text{-btapa})_2(\text{NO}_3)_2] \cdot 6\text{H}_2\text{O} \cdot 2\text{DMF}\}_n$

Source: Hasegawa, S., Horike, S., Matsuda, R., Furukawa, S., Mochizuki, K., Kinoshita, Y., Kitagawa, S., *J. Am. Chem. Soc.*, 129(9) (2007), 2607–2614

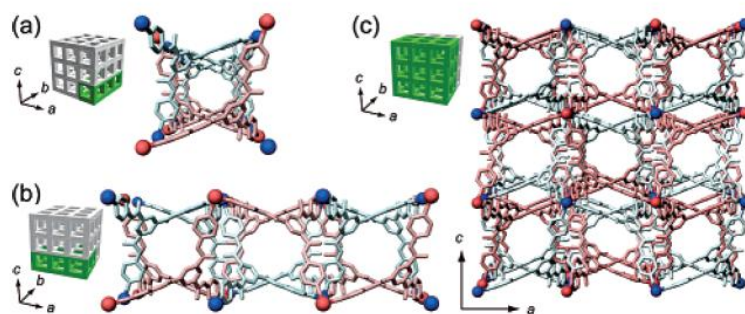


Fig.10. Two-fold interpenetrating 3D crystal structure of $\{[\text{Cd}(4\text{-btapa})_2(\text{NO}_3)_2] \cdot 6\text{H}_2\text{O} \cdot 2\text{DMF}\}_n$ to form three-dimensionally channels

Source: Hasegawa, S., Horike, S., Matsuda, R., Furukawa, S., Mochizuki, K., Kinoshita, Y., Kitagawa, S., *J. Am. Chem. Soc.*, 129(9) (2007), 2607–2614

The Knoevenagel condensation reaction was performed using the benzaldehyde and three methylene compounds (malononitrile, ethyl cyanoacetate and cyano-acetic acid *tert*-butyl ester) with the $\{[\text{Cd}(4\text{-btapa})_2(\text{NO}_3)_2] \cdot 6\text{H}_2\text{O} \cdot 2\text{DMF}\}_n$ as catalyst [11]. The obtained data can be seen in Table 1.

Table 1. Knoevenagel condensation catalytic test of $\{[\text{Cd}(4\text{-btapa})_2(\text{NO}_3)_2] \cdot 6\text{H}_2\text{O} \cdot 2\text{DMF}\}_n$

Run	Substrate	Molecular size (Å)	Conversion (%)
1	Malononitrile	6.9 x 4.5	98
2	ethyl cyanoacetate	10.3 x 4.5	7
3	cyano-acetic acid <i>tert</i> -butyl ester	10.3 x 5.8	0

Source: Hasegawa, S., Horike, S., Matsuda, R., Furukawa, S., Mochizuki, K., Kinoshita, Y., Kitagawa, S., *J. Am. Chem. Soc.*, 129(9) (2007), 2607–2614

From the conversion values and molecular sizes can be concluded that the reaction takes place within the channels and not on the surface of the catalyst. In the case of the malononitrile a conversion of 98% was obtained due to the fact that its size (6.9 x 4.5 Å) is similar to the dimensions of the channel - 4.7 x 7.3 Å, while for the other two substrates their sizes are bigger and cannot fit properly or fitting in the channels.

2.1.2. Incorporation of nanocatalysts

When incorporating metal nanoparticles into coordination polymers as support, the walls of PCPs framework will apply a constrain confining and restricting the growth of the nanoparticles. El-Shall et al. [12] conducted a study in which they incorporated Pd, Cu and Pd-Cu nanoparticles, respectively, into MIL-101, a chromium-based metal-organic framework, and performed the carbon monoxide catalytic oxidation.

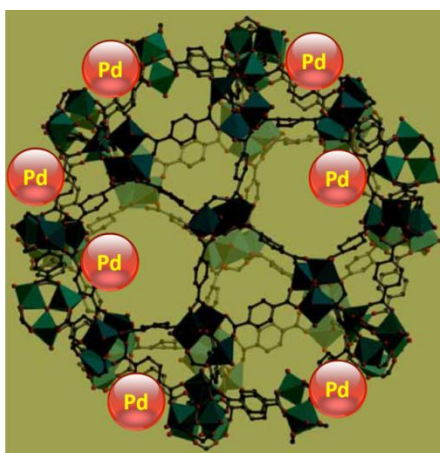


Fig.11. Graphic representation of palladium nanoparticles supported on MIL-101

Source: El-Shall, M.S., Abdelsayed, V., Khder, A.E.R.S., Hassan, H.M.A., El-Kaderi, H.M., Reich, T.E., *J. Mater. Chem.*, 19(41) (2009), 7625–7631

The MIL-101 supported nanocatalysts were obtained using two methods, based on the simultaneous activation of the pores of MIL-101 and the rapid chemical reduction of the metal precursors using hydrazine and microwave irradiation [12].

The first method consists in the addition of metal nitrate to an aqueous dispersion of MIL-101, followed by the addition of hydrazine and heating with microwave irradiation. In the second method, the MIL-101 was stirred in the nitrate solution, separated by centrifugation, and then it was redispersed in water following the addition of hydrazine and

heating with microwave irradiation [12]. Through the first method higher loadings of nanoparticles were obtained.

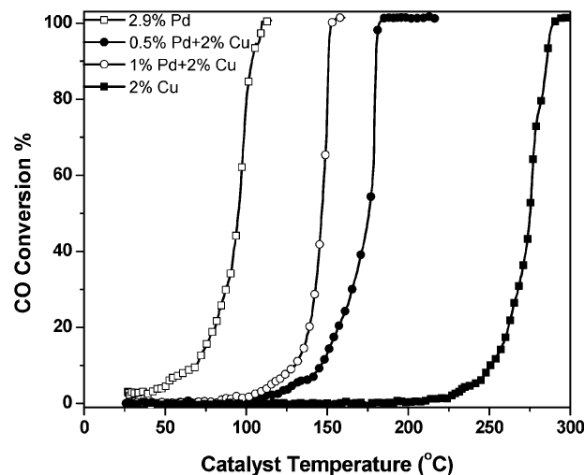


Fig.12. CO oxidation on Pd, Cu, and mixed Pd–Cu nanocatalysts supported on MIL-101
Source: El-Shall, M.S., Abdelsayed, V., Khder, A.E.R.S., Hassan, H.M.A., El-Kaderi, H.M., Reich, T.E., *J. Mater. Chem.*, 19(41) (2009), 7625–7631

In Figure 12 it can be seen that Pd nanoparticles doped MIL-101 shows the best catalytic activity and decreasing in the case of the Pd-Cu doped MIL-101 with the decrease of the Pd%. Figure 13 compares the catalytic activity of MIL-101 supported nanocatalyst having different palladium loading percentages, prepared using both methods, as well as the simple free MIL-101. Pd (2.9%)-MIL catalyst exhibits the best catalytic activity with a full conversion at 107 °C [12].

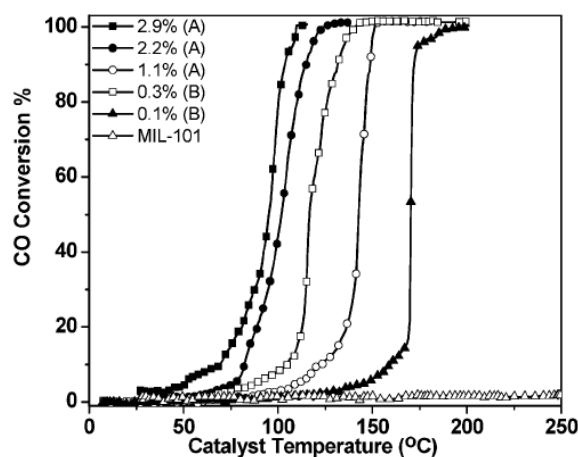


Fig.13. CO oxidation on Pd nanoparticles-doped MIL-101
Source: El-Shall, M.S., Abdelsayed, V., Khder, A.E.R.S., Hassan, H.M.A., El-Kaderi, H.M., Reich, T.E., *J. Mater. Chem.*, 19(41) (2009), 7625–7631

2.1.3. Immobilization of unsaturated metal sites

Chen *et al.* obtained a chromium-based porous coordination polymer having unsaturated chromium ions by using an isophthalic acid ligand modified with sulfonic groups. The compound was used as an acid catalyst to transform glucose into 5-hydroxymethylfurfural (HMF) in a biomass recovery process due to the fact that is representing a renewable and sustainable alternative to fossil resources [13].

The PCP(Cr)-SO₃H•Cr(III) catalyst was prepared using a hydrothermal method by self-assembly of monosodium 5-sulfoisophthalate with metal ions [13].

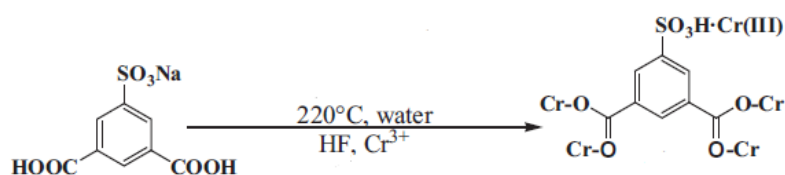


Fig.14. Synthetic route of PCP(Cr)-SO₃H•Cr(III)

Source: Chen, D., Liang, F., Feng, D., Xian, M., Zhang, H., Liu, H., Du, F., Chem. Eng. J., 300 (2016), 177–184

In Table 2 it can be seen the conversion of glucose and fructose to HMF using different systems. Even though the highest result was obtained for the fructose conversion in DMSO, with a HMF yield of 95%, the best system proved to be the biphasic salted water/THF system as both glucose and fructose were converted with high yields, of 80.7% and 85.3% respectively.

Table 2. Conversion of glucose and fructose to HMF in different solutions

Entry	Feed	System	HMF yield (%)
1	Glucose	DMSO	9.3
2	Fructose	DMSO	95.0
3	Glucose	THF	9.8
4	Glucose	Water	49.7
5	Glucose	Water/THF	21.6
6	Glucose	Water/THF/NaCl	80.7
7	Fructose	Water/THF/NaCl	85.3

Source: Chen, D., Liang, F., Feng, D., Xian, M., Zhang, H., Liu, H., Du, F., Chem. Eng. J., 300 (2016), 177–184

In Figure 15 it can be observed the influence of the catalyst amount, the water to THF ratio, temperature, and time on the glucose transformation into HMF. The proper system

needed to obtain the highest HMF yield consists in a water to THF ratio of 1:2 with 75 mg of catalyst. At the temperature of 180-190 °C the HMF yield of 80.7% is achieved with a full conversion of glucose and the highest HMF selectivity values. This catalytic performance can be observed in plot (d) after 4 hours of reaction time.

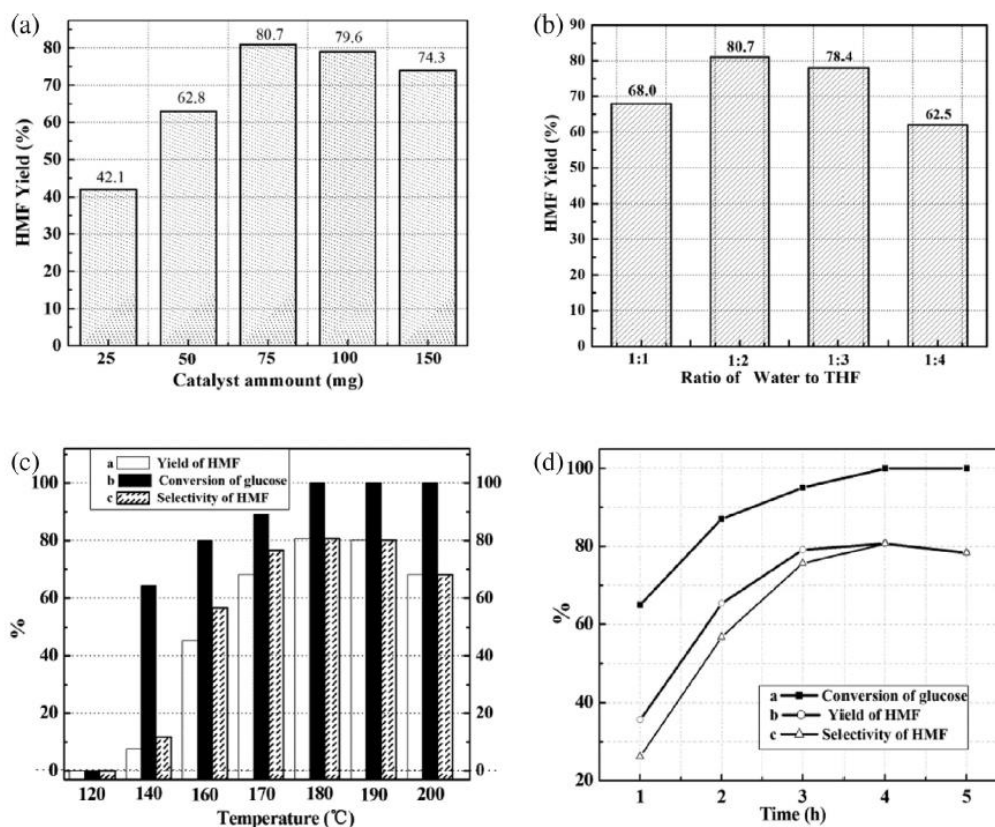


Fig.15. Catalyst amount (a), water to THF ratio (b), temperature (c), time (d) effects on glucose-to-HMF transformation

Source: Chen, D., Liang, F., Feng, D., Xian, M., Zhang, H., Liu, H., Du, F., Chem. Eng. J., 300 (2016), 177–184

2.2. Gas storage

Due to their adsorption properties, determined by their structural features, porous coordination polymers were rapidly recognized as gas storage and separation materials. Kitagawa *et al.* were the first to report the methane adsorption in 1997-2000, using three-dimensional frameworks build from 4,4'-bpy linkers and M(II) = Co, Ni, Zn connectors and in 2003, the first hydrogen storage measurements performed on isorecticular MOF-5 and IRMOF-8 were reported by Yaghi *et al* [8,14].

Porous coordination polymers exhibit high gravimetric and volumetric storage capacity and also a stronger interaction with the gas molecules [14], which gives an

advantage to these compounds over the other porous materials. However, the most important feature for a higher uptake of gas molecules is the pores size, influencing the gas storage at both high and low pressures [8]. When pores dimensions are closer to the sizes of the gas molecules a stronger interaction will be formed which will lead to a better adsorption of the guest into the pores.

Nowadays, heavy industry and the chemicals production are causing negative effects on both the environment and our society, leading to high atmospheric pollution, consumption of resources and the increase of the ever-present greenhouse effect. As such, a better control or even a decrease of these effects is mandatory and this can be achieved with the use of metal organic frameworks to alleviate the greenhouse effect caused by the carbon dioxide, to control the toxic gases, such as carbon monoxide, ammonia and hydrogen sulfide and to widespread the clean energy through the use of energy-related gases (hydrogen and low molecular weight hydrocarbons) [15].

2.2.1. Carbon dioxide storage

Large amounts of carbon dioxide occur during the combustion of fossil fuels for the energy production. PCPs separate and capture the carbon dioxide from the gas mixture based on the different interaction of gas molecules with the frameworks.

CO₂ capture using PCPs are performed in the following situation: post-combustion capture, pre-combustion capture, oxy-fuel combustion, and direct capture from air. In the post-combustion capture, carbon dioxide is absorbed at low pressure, usually atmospheric pressure, while in the pre-combustion capture the fuels must first undergo decarbonation and the carbon dioxide is adsorbed at high pressures (5-40 bars) in order to obtain zero CO₂ during the combustion step. Oxy-fuel combustion implies the use of nearly pure O₂ and will result in almost completely CO₂ generated gas, after the removal of water, thus facilitating the capture step [15].

De *et al.* synthesized two isostructural porous coordination polymers using a linear tetracarboxylic acid ligand, decorated with amino groups, and zinc or copper nitrates, respectively. The Cu-MOF, {[Cu₂ (ATPTA) (H₂O)₂]}_n, proved to be more stable and allows the removal of the solvent molecules leading to a high porous surface and therefore was tested for the gas adsorption properties using hydrogen, methane and carbon dioxide [16].

The structure of the ligand as well as the Cu²⁺ ions environment can be seen in Figure 16. The terphenyl core confers a high rigidity to the final structure and the amino group acts

as guest interaction site. The two copper ions are pentacoordinated, adopting a square-pyramidal geometry with an oxygen atom in the apex of the pyramid and four ligands are linking the two ions via carboxylate bridges. In Figure 16 (d), it can be observed a view along the *c* crystallographic axis revealing two types of pores in the compounds.

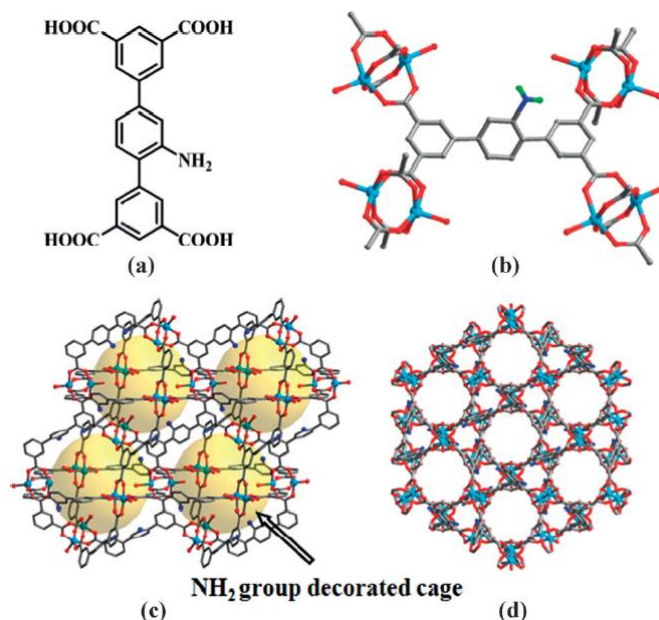


Fig.16. Structure of ATPTA ligand (a), coordination environment of Cu²⁺, NH₂ decorated cages (c) and pore structures (d) of {[Cu₂(ATPTA)(H₂O)₂]}_n

Source: De, D., Pal, T.K., Neogi, S., Senthilkumar, S., Das, D., Gupta, S.S., Bharadwaj, P.K., Chem.: Eur. J., 22(10) (2016), 3387–3396

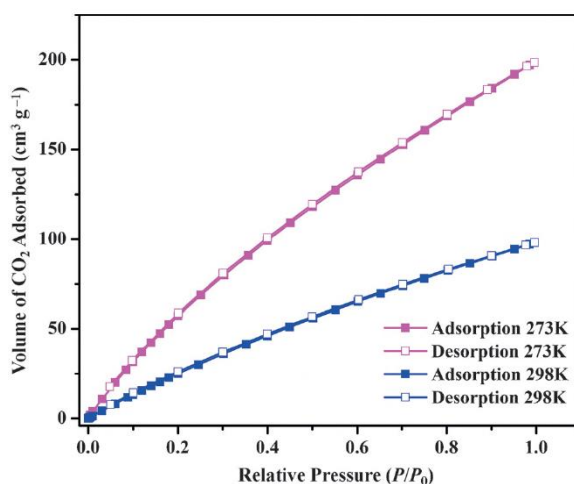


Fig.17. CO₂ adsorption and desorption isotherms for {[Cu₂(ATPTA)(H₂O)₂]}_n at 273 and 298 K

Source: De, D., Pal, T.K., Neogi, S., Senthilkumar, S., Das, D., Gupta, S.S., Bharadwaj, P.K., Chem. Eur. J., 22(10) (2016), 3387–3396

Figure 17 shows the carbon dioxide adsorption and desorption isotherms at 0 and 25 °C. At atmospheric pressure and room temperature, the CO₂ adsorption capacity of {[Cu₂(ATPTA)(H₂O)₂]_n reaches the values of approximately 90 cm³g⁻¹ and with the decrease of temperature the adsorbed CO₂ volume increases reaching almost 200 cm³g⁻¹ at 0 °C.

2.2.2. Hydrogen storage

Hydrogen is an excellent alternative for coal and gasoline because of its ultrahigh gravimetric combustion heat and benign combustion products and could improve the environment if it would be used as fuel for automobiles. Two techniques are exploited for the hydrogen storage with the use of porous coordination polymers: cryo-temperature storage which implies the retaining of hydrogen in a tank filled with PCPs at usually 77 K and relatively low pressure (below 100 bars) and the room-temperature storage. Because of the weak interactions with the surface of the PCPs at room temperature the hydrogen adsorption does not work efficiently [15].

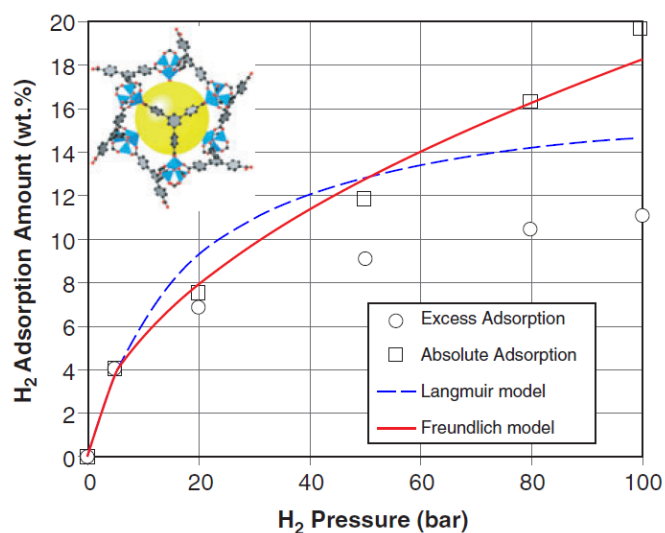


Fig.18. Hydrogen adsorption plot of MOF-177 at high pressure and 77 K, displaying the excess, absolute, Langmuir and Freundlich adsorption

Source: Peedikakkal A.M.P., Adarsh N.N., Porous Coordination Polymers in Jafar Mazumder M., Sheardown H., Al-Ahmed A. (eds) Functional Polymers. Polymers and Polymeric Composites: A Reference Series. Springer, Cham (2019)

In Figure 18 is depicted the hydrogen adsorption plot of MOF-177 at high pressure and 77 K, displaying the excess, absolute, Langmuir and Freundlich adsorption.

2.2.3. Hydrocarbons storage

Hydrocarbons adsorption by porous coordination polymers takes place via van der Waals interactions between the hydrocarbons and the frameworks and also uses of the flexibility of the PCPs for a better uptake depending on the hydrocarbon concentrations [15]. Besides hydrogen, methane is another fuel alternative due to its low carbon emission and thermal efficiency and also because of its abundance, being the major component of natural gas [17]. Due to its potential, many studies focused on the methane adsorption using different PCP architectures.

Acetylene is the simplest alkyne and is widely used as gas for oxy-acetylene welding and metal cutting and is a key starting material for electronic materials, as well as in manufacturing of various fine chemicals, such as vinyl chloride and methyl acrylate [17].

Methane adsorption

Jiang *et al.* [18] obtained a series of MOF materials based on the Zn_4O cluster and H_3BTAC ligand and a series of functionalized H_2DBC linkers: MOF-905, MOF-905- Me_2 , MOF-905-Naph, MOF-905- NO_2 and MOF-950 and performed the methane adsorption of these materials at both low and high pressure and room temperature. MOF-905 is built with use of the H_2DBC linker and presents two types of cages in its structure: octahedral (yellow) and tetrahedral (green) cages, which can be observed in Figure 19.

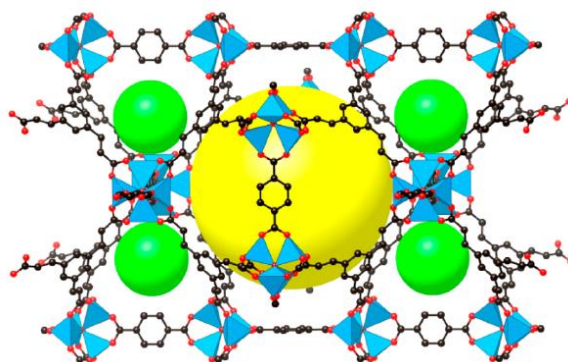


Fig.19. Structure of MOF-905 with the octahedral (yellow) and tetrahedral (green) cages

Source: Jiang, J., Furukawa, H., Zhang, Y.-B., Yaghi, O.M., *J. Am. Chem. Soc.*, 138(32) (2016), 10244–10251

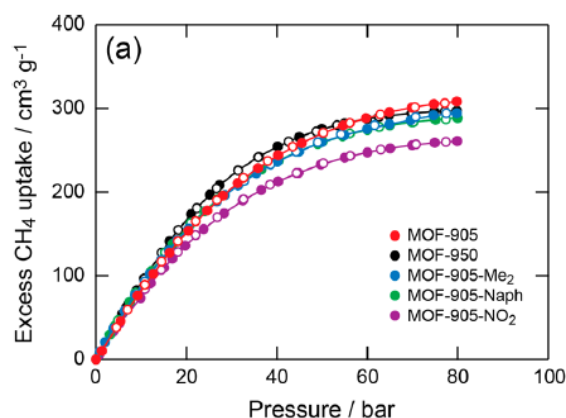
The low-pressure adsorption of this series of materials was performed at 1.1 bar and it can be observed in Table 3 that none of them has a significant methane uptake, the values being in the range of $7.7\text{--}11.0\text{ cm}^3\text{g}^{-1}$.

Table 3. Low-pressure methane adsorption of different MOFs at 1.1 bar and 298 K

Material	Surface area (cm ² g ⁻¹)		CH ₄ uptake (cm ³ g ⁻¹)
	BET	Langmuir	
MOF-905	3490	3770	7.7
MOF-905-Me ₂	3640	3920	11.0
MOF-905-Naph	3310	3540	10.2
MOF-905-NO ₂	3380	3600	8.1
MOF-950	3440	3650	8.6

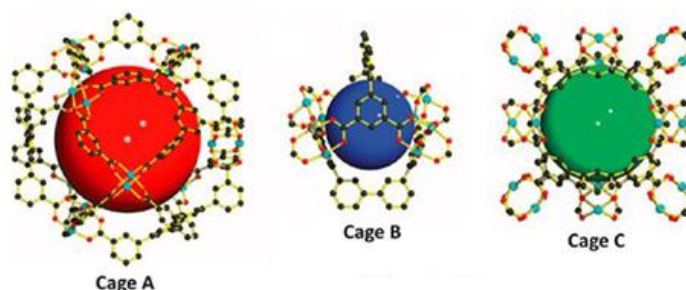
Source: Jiang, J., Furukawa, H., Zhang, Y.-B., Yaghi, O.M., J. Am. Chem. Soc., 138(32) (2016), 10244–10251

When increasing the pressure up to 80 bar the methane uptake increases considerably for all materials reaching its highest in the case of MOF-905 with a value of 310 cm³g⁻¹ [18], which is about 39 times bigger than the low-pressure adsorption (Figure 20).

**Fig.20.** High-pressure methane adsorption of different MOFs at 298 K

Source: Jiang, J., Furukawa, H., Zhang, Y.-B., Yaghi, O.M., J. Am. Chem. Soc., 138(32) (2016), 10244–10251

Acetylene adsorption

**Fig.21.** Three different cage types in FJI-H8

Source: He, Y., Chen, F., Li, B., Qian, G., Zhou, W., Chen, B., Coord. Chem. Rev., 373 (2018), 167–198.

FJI-H8 is a porous coordination polymer obtained by Yuan *et al.* in 2015 showing high acetylene uptake at ambient conditions. This compound is based on copper clusters and isophthalate ligands that give rise to an architecture having three types of nanocages, which can be observed in Figure 21. Cage A represents a cuboctahedral with a pore diameter of 15 Å, cage B is a distorted octahedral with a pore dimension of 8 Å and cage C is a distorted cuboctahedral having a pore diameter of 12 Å [17].

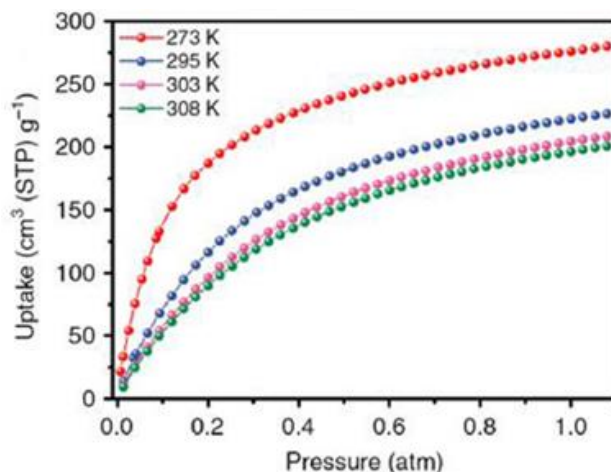


Fig.22. Acetylene adsorption isotherms of FJI-H8 at four different temperatures
Source: He, Y., Chen, F., Li, B., Qian, G., Zhou, W., Chen, B. *Coord. Chem. Rev.*, 373 (2018), 167–198.

In Figure 22 it can be seen the acetylene adsorption of FJI-H8 at the temperatures of 273, 295, 303 and 308 K respectively. At 0 °C the maximum uptake is achieved, around 280 cm³g⁻¹ and also show a very good uptake at room temperature, around 220 cm³g⁻¹.

2.2.4. Toxic gases storage

The separation and storage of toxic gases, such as carbon monoxide, nitrogen oxides, ammonia, sulfur dioxide, and hydrogen sulfide are related to human health and chemical production [15]. The ammonia and hydrogen sulfide adsorption using porous coordination polymers will be presented in the following part.

Ammonia adsorption

Leroux *et al.* obtained a Cd based porous coordination polymer with pyridinium carboxylate ligands (pc1) having the formula {[Cd₄Cl₆(pc1)₆]CdCl₄}_n. The compound has tetrameric building blocks that generate hexagonal channels in the final structure of the

compounds [19], which can be observed in Figure 23. Also, in the inset, the interaction of water molecules with the framework's walls can be seen.

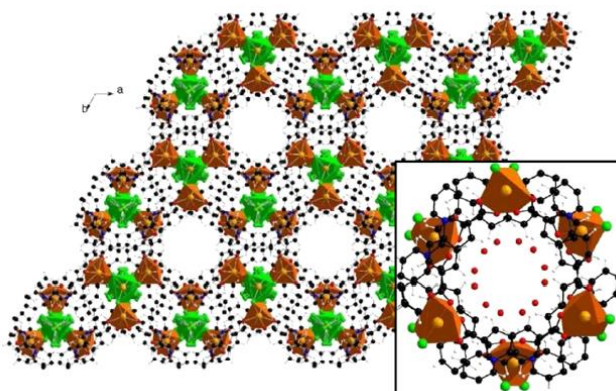


Fig.23. The general view of $\{[\text{Cd}_4\text{Cl}_6(\text{pc1})_6]\text{CdCl}_4\}_n$ showing hexagonal channels
Source: Leroux, M., Mercier, N., Allain, M., Dul, M.-C., Dittmer, J., Kassiba, A.H., Bezverkhyy, I.,
Inorg. Chem., 55(17) (2016), 8587–8594

The synthesized compound presents a high ammonia uptake at room temperature, reaching a maximum of 22.8 mmol/g at 900 hPa which corresponds to 0.39 g of ammonia per 1 g of compound [19].

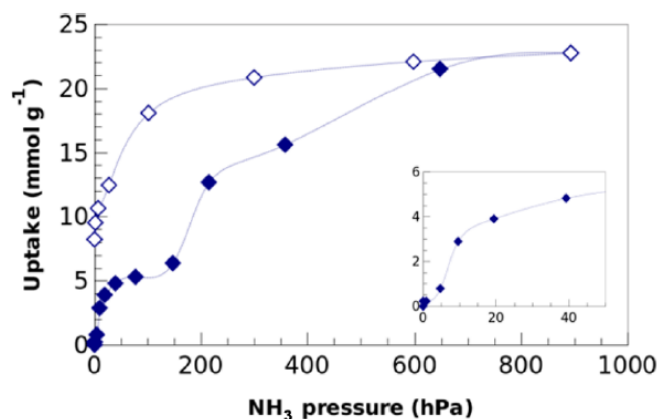


Fig.24. Ammonia adsorption and desorption isotherms of $\{[\text{Cd}_4\text{Cl}_6(\text{pc1})_6]\text{CdCl}_4\}_n$
Source: Leroux, M., Mercier, N., Allain, M., Dul, M.-C., Dittmer, J., Kassiba, A.H., Bezverkhyy, I.,
Inorg. Chem., 55(17) (2016), 8587–8594

Hydrogen sulfide adsorption

Belmabkhout *et al.* developed a series of isostructural metal-organic framework with square-octahedral topology (soc-MOF), having the general formula $\{[\text{M}_3\text{O}(\text{ABTC})_6]\}_n$, using azobenzene tetracarboxylic acid (ABTC) linking groups and different oxo-centered trinuclear metal cluster ($\text{M} = \text{In}^{3+}, \text{Fe}^{3+}, \text{Ga}^{3+}, \text{Al}^{3+}$). They performed the gas adsorption on this

compounds using carbon dioxide and different hydrocarbons such as methane (CH_4), ethane (C_2H_6), ethylene (C_2H_4), propane (C_3H_8) and propylene (C_3H_6) and also succeeded to perform the hydrogen sulfide adsorption on the gallium based metal-organic framework [20].

The general structure of the $\{[\text{M}_3\text{O}(\text{ABTC})_6]\}_n$ compounds can be seen in Figure 25.

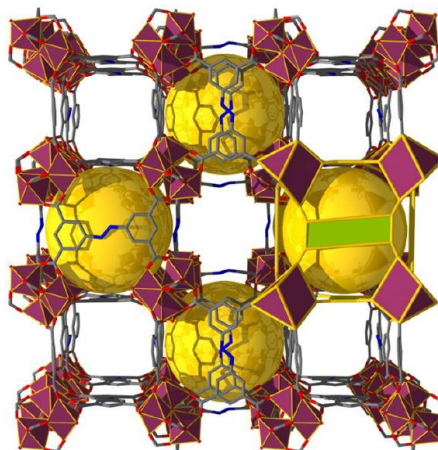


Fig.25. Structure of $\{[\text{M}_3\text{O}(\text{ABTC})_6]\}_n$ compounds

Source: Belmabkhout, Y., Pillai, R.S., Alezi, D., Shekhah, O., Bhatt, P.M., Chen, Z., Eddaoudi, M., *J. Mater. Chem. A*, 5(7) (2017), 3293–3303

Figure 26 shows the comparison between the hydrogen sulfide adsorption performed on $\{[\text{Ga}_3\text{O}(\text{ABTC})_6]\}_n$ at room temperature and the collected data for the methane and carbon dioxide adsorption. It can be seen that the hydrogen sulfide exhibits the highest affinity toward the compound, which can be explained by the favorable binding of H_2S to the exposed and coordinatively unsaturated gallium open metal sites [20].

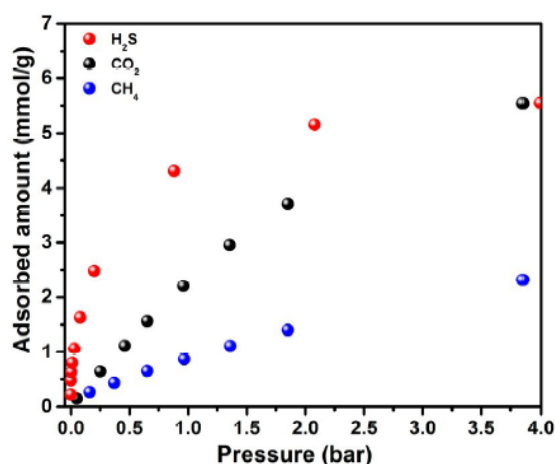


Fig.26. Hydrogen sulfide, carbon dioxide and methane adsorption on $\{[\text{Ga}_3\text{O}(\text{ABTC})_6]\}_n$

Source: Belmabkhout, Y., Pillai, R.S., Alezi, D., Shekhah, O., Bhatt, P.M., Chen, Z., Eddaoudi, M., *J. Mater. Chem. A*, 5(7) (2017), 3293–3303

Objectives of the MSc Thesis

The main objectives that we have proposed to develop in the MSc thesis are:

- To synthesize and characterize a number of copper-based porous coordination polymers in terms of catalytic and gas storage properties.
- To evaluate the influence of different ligands on the capacity of gases adsorption.
- To investigate the catalytic properties of the obtained porous compounds.
- To enlarge this series with new compounds that may have similar or even enhanced catalytic and gas storage properties.

References

1. Zhou, H.-C., Long, J.R., Yaghi, O.M., Introduction to Metal–Organic Frameworks. *Chem. Rev.*, 112(2) (2012), 673-674.
2. Bu, F.-X., Hu, M., Xu, L., Meng, Q., Mao, G.-Y., Jiang, D.-M., Jiang, J.-S., Coordination polymers for catalysis: enhancement of catalytic activity through hierarchical structuring. *Chem. Commun.*, 50(62) (2014), 8543-8546.
3. Janiak, C., Vieth, J.K. MOFs, MILs and more: concepts, properties and applications for porous coordination networks (PCNs). *New J. Chem.*, 34(11) (2010), 2366-2388.
4. Sánchez-Serratos, M., Álvarez, J.R., González-Zamora, E., Ibarra, I.A., Porous Coordination Polymers (PCPs): New Platforms for Gas Storage. *J. Mex. Chem. Soc.*, 60(2) (2016), 43-57.
5. Robin, A.Y., Fromm, K.M., Coordination polymer networks with O- and N-donors: What they are, why and how they are made. *Coord. Chem. Rev.*, 250(15-16) (2006), 2127–2157.
6. Seo, J., Sakamoto, H., Matsuda, R., Kitagawa, S., Chemistry of Porous Coordination Polymers Having Multimodal Nanospace and Their Multimodal Functionality. *J. Nanosci. Nanotechnol.*, 10(1) (2010), 3–20.
7. Hönicke, I., Senkovska, I., Bon, V., Baburin, I., Boenisch, N., Raschke, S., Kaskel, S., Balancing Mechanical Stability and Ultrahigh Porosity in Crystalline Framework Materials, *Angew. Chem. Int. Ed.*, 57(42) (2018), 13780-13783
8. Bon, V., Senkovska, I., Kaskel, S., Chapter 6: Metal-Organic Frameworks in K. Kaneko, F. Rodríguez-Reinoso (eds.), *Nanoporous Materials for Gas Storage, Green Energy and Technology*, Ed. Springer, Singapore, (2019) 137–172.
9. Bureekaew, S., Shimomura, S., Kitagawa, S., Chemistry and application of flexible porous coordination polymers, *Sci. Technol. Adv. Mater.*, 9(1) (2008), 014108-014119.
10. Ghosh, A., Hazra, A., Mondal, A., Banerjee, P. Weak interactions: the architect behind the structural diversity of coordination polymer. *Inorg. Chim. Acta*, 488 (2019), 86-119.

11. Hasegawa, S., Horike, S., Matsuda, R., Furukawa, S., Mochizuki, K., Kinoshita, Y., Kitagawa, S., Three-Dimensional Porous Coordination Polymer Functionalized with Amide Groups Based on Tridentate Ligand: Selective Sorption and Catalysis. *J. Am. Chem. Soc.*, 129(9) (2007), 2607–2614.
12. El-Shall, M.S., Abdelsayed, V., Khder, A.E.R.S., Hassan, H.M.A., El-Kaderi, H.M., Reich, T.E., Metallic and bimetallic nanocatalysts incorporated into highly porous coordination polymer MIL-101. *J. Mater. Chem.*, 19(41) (2009), 7625–7631.
13. Chen, D., Liang, F., Feng, D., Xian, M., Zhang, H., Liu, H., Du, F., An efficient route from reproducible glucose to 5-hydroxymethylfurfural catalyzed by porous coordination polymer heterogeneous catalysts. *Chem. Eng. J.*, 300 (2016), 177–184.
14. Peedikakkal A.M.P., Adarsh N.N., Porous Coordination Polymers in Jafar Mazumder M., Sheardown H., Al-Ahmed A. (eds) *Functional Polymers. Polymers and Polymeric Composites: A Reference Series*. Springer, Cham (2019)
15. Li, H., Wang, K., Sun, Y., Lollar, C.T., Li, J., Zhou, H.-C., Recent advances in gas storage and separation using metal–organic frameworks. *Mater. Today*, 21(2) (2018), 108–121.
16. De, D., Pal, T.K., Neogi, S., Senthilkumar, S., Das, D., Gupta, S.S., Bharadwaj, P.K., A Versatile Cu^{II} Metal-Organic Framework Exhibiting High Gas Storage Capacity with Selectivity for CO₂: Conversion of CO₂ to Cyclic Carbonate and Other Catalytic Abilities. *Chem.: Eur. J.*, 22(10) (2016), 3387–3396.
17. He, Y., Chen, F., Li, B., Qian, G., Zhou, W., Chen, B., Porous metal–organic frameworks for fuel storage. *Coord. Chem. Rev.*, 373 (2018), 167–198.
18. Jiang, J., Furukawa, H., Zhang, Y.-B., Yaghi, O.M., High Methane Storage Working Capacity in Metal–Organic Frameworks with Acrylate Links. *J. Am. Chem. Soc.*, 138(32) (2016), 10244–10251.
19. Leroux, M., Mercier, N., Allain, M., Dul, M.-C., Dittmer, J., Kassiba, A.H., Bezverkhy, I., Porous Coordination Polymer Based on Bipyridinium Carboxylate Linkers with High and Reversible Ammonia Uptake. *Inorg. Chem.*, 55(17) (2016), 8587–8594.
20. Belmabkhout, Y., Pillai, R.S., Alezi, D., Shekhah, O., Bhatt, P.M., Chen, Z., Eddaoudi, M., Metal–organic frameworks to satisfy gas upgrading demands: fine-tuning the soc-MOF platform for the operative removal of H₂S. *J. Mater. Chem. A*, 5(7) (2017), 3293–3303.